Native defect properties and *p*-type doping efficiency in group-IIA doped *wurtzite* AlN

Yong Zhang,[1,2] Wen Liu,[2] and Hanben Niu[2,*]

[1]*Institute of Optoelectronics Science and Engineering, Huazhong University of Science and Technology, Wuhan 430074, China*

[2]*Institute of Optoelectronics and Key Laboratory of Optoelectronic Devices and Systems of Ministry of Education, Shenzhen University, Shenzhen 518060, China*

(Received 18 April 2007; published 2 January 2008)

Using the first-principles full-potential linearized augmented plane-wave (FPLAPW) method based on density functional theory (DFT), we have investigated the native defect properties and *p*-type doping efficiency in AlN doped with group-IIA elements such as Be, Mg, and Ca. It is shown that nitrogen vacancies (V_N) have low formation energies and introduce deep donor levels in *wurtzite* AlN, while in *zinc blende* AlN and GaN, these levels are reported to be shallow. The calculated acceptor levels $\epsilon(0/-)$ for substitutional Be (Be_{Al}), Mg (Mg_{Al}), and Ca (Ca_{Al}) are 0.48, 0.58, and 0.95 eV, respectively. In *p*-type AlN, Be interstitials (Be_i), which act as donors, have low formation energies, making them a likely compensating center in the case of acceptor doping. Whereas, when N-rich growth conditions are applied, Be_i are energetically not favorable. It is found that *p*-type doping efficiency of substitutional Be, Mg, and Ca impurities in *w*-AlN is affected by atomic size and electronegativity of dopants. Among the three dopants, Be may be the best candidate for *p*-type *w*-AlN. N-rich growth conditions help us to increase the concentration of Be_{Al}, Mg_{Al}, and Ca_{Al}.

DOI: 10.1103/PhysRevB.77.035201 PACS number(s): 61.72.Bb, 61.72.J−, 61.72.uj, 71.15.Nc

I. INTRODUCTION

Group-III nitrides (III-N, III=Ga, Al, and In) are wide-gap semiconductors and have attracted researcher's attention for more than two decades due to their promising applications for the blue-ultraviolet (UV) optoelectronics.[1–5] Among all III-V nitrides, *wurtzite* AlN has the widest direct gap (varies from 6.28 eV at 5 K to 6.2 eV at room temperature).[6] Thus, to push the optical emission and/or detection wavelength to the deep UV region ($\lambda \sim 200$ nm), AlN is of great interest.

In spite of the recognition of the importance of AlN, the report of light emitting directly from AlN is rare due to the lack of high-quality films. Recently, Taniyasu *et al.* have reported a light emitter with 210 nm made of AlN doped with Si and Mg, which is the shortest wavelength emitted by light-emitting diode at present,[7] whereas the internal quantum efficiency is still low due to low *p*-type doping efficiency. So the fabrication of *p*-type doped layers is essential for all of these devices. However, similar to GaN, the growth of highly conductive *p*-type AlN layers has so far proven to be difficult. The main reasons have been proposed to be the formation of donor defects, such as nitrogen vacancies, limited dopant solubility, and deep acceptor energy levels. Following the "doping limit rule,"[8] it will be much more difficult to achieve *p*-type AlN than to achieve *p*-type GaN.

To exploit fully the potential of AlN, systematic studies of native defects and impurities in AlN are required. While there have been several theoretical and experimental studies of crystal defects in GaN,[9–11] little work has been done on AlN. Magnesium is commonly used as *p*-type dopant for nitride semiconductors, but the Mg low doping efficiency is due to the deep acceptor level introduced by Mg. It would be desirable to find an alternative dopant that would exhibit higher solubility and lower ionization energy. In Ref. 7, group-II and -IV elements have been proposed to be potential candidates for Mg. However, group-IV elements are likely to become donors when incorporated in the cation sites, which will result in severe self-compensation.[12] Thus, group-II elements may be better candidates than group-IV elements for *p*-type AlN doping. In GaN, it has been reported that the acceptor level of Be_{Ga} is shallower than that of Mg_{Ga}. However, the behavior of doping Be in *w*-AlN is still unclear. To improve *p*-type doping efficiency, systemic studies of doping properties of group-IIA elements in AlN are important.

In this work, theoretical studies are performed to understand the configurations of native defects and substitutional Be, Mg, and Ca impurities in *wurtzite* AlN. By comparing the formation energies and transition levels of Be-, Mg-, and Ca-related defects, the *p*-type doping efficiency of these dopants is examined. The organization of this paper is as follows. In Sec. II, the computational methods are introduced. Section III gives some discussion and results. Section IV summarizes the paper and contains some suggestions for future experimental work.

II. METHODS

The calculations are performed using the FPLAPW method implemented in WIEN2K package.[13] The generalized gradient approximation of Perdew-Burke-Ernzerhof 96 (Ref. 14) is employed for the exchange-correlation potential. Calculations were done with $R_{MT}K_{max}=9$ (where R_{MT} is the average radius of the muffin-tin spheres and K_{max} is the maximum modulus for the reciprocal lattice vector). The iteration process was repeated until the calculated total energy difference between succeeding iterations is less than 0.1 mRy and the force on each atom is less than 1.0 mRy/a.u. To simulate isolated defects, a 72-atom AlN supercell consisting of $3\times3\times2$ primitive *wurtzite* cells is used as it was found to be adequate in earlier work on similar systems.[15] The $4\times4\times3$ *k*-point mesh produces converged results. The lattice parameters of supercell are fixed and are described by

the theoretical value of pure AlN. The theoretical band gap derived from the band structure is ~4.1 eV and about 2.0 eV below the experimental gap. To find a realistic description of both defect levels and band edges, we obtain them both from electron addition and removal calculations. The theoretical band gap evaluated from $E^{-}[R(-)]+E^{+}[R(+)]-2E^{0}[R(0)]$ (Ref. 16) is 5.98 eV, in acceptable agreement with the experimental value of 6.12 eV.[17]

At equilibrium and in the dilute limit, the concentration of a defect in a crystal depends upon its formation energy E^f. Following Van de Walle and Neugebauer,[18] the formation energy of a defect or impurity X (X=Be, Mg, and Ca in present work) in charge state q is calculated from

$$E^f(X^q) = E_{tot}[X^q] - E_{tot}[\mathrm{AlN}, bulk] - \sum n_i\mu_i + q[E_F + E_V + \Delta V], \quad (1)$$

where $E_{tot}[X^q]$ is the total energy of the defect-containing AlN supercell and $E_{tot}[\mathrm{AlN}, bulk]$ is the total energy of the equivalent supercell of AlN containing no defects. Here, n_i indicates the number of atoms that have been added to ($n_i>0$) or removed from ($n_i<0$) the supercell and μ_i are the corresponding chemical potentials of these species. E_F is the Fermi level, referenced to the valence-band maximum E_V in the bulk. A correction term ΔV is used to align the reference potential in our defect supercell with that in the bulk.

The chemical potentials μ depend on growth process.[19] To determine the bound of μ_{Al} and μ_X, we compute the enthalpy of formation of AlN and X_3N_2 assuming the formation from metallic Al, X, and gaseous N_2 ($\Delta H_f[\mathrm{AlN}]=-2.06$ eV, $\Delta H_f[X_3N_2]=-5.0$, -3.36, and -2.63 eV for X=Be, Mg, and Ca, respectively). Chemical potentials are calculated using the following relationships:

$$\mu_{\mathrm{Al}} + \mu_{\mathrm{N}} = \mu_{\mathrm{AlN}} = \mu_{\mathrm{Al[bulk]}} + \mu_{\mathrm{N[N_2]}} + \Delta H_f[\mathrm{AlN}], \quad (2)$$

$$3\mu_X + 2\mu_{\mathrm{N}} = \mu_{X_3N_2} = 3\mu_{X[\mathrm{bulk}]} + 2\mu_{\mathrm{N[N_2]}} + \Delta H_f[X_3N_2]. \quad (3)$$

By combining Eqs. (2) and (3), the chemical potential of Al and impurity X are therefore

$$\mu_{\mathrm{Al}} = \mu_{\mathrm{Al[bulk]}}, \quad (4)$$

$$\mu_X = \mu_{X[\mathrm{bulk}]} + \frac{1}{3}\Delta H_f[X_3N_2] - \frac{2}{3}\Delta H_f[\mathrm{AlN}], \quad (5)$$

for Al-rich limit, and

$$\mu_{\mathrm{Al}} = \mu_{\mathrm{Al[bulk]}} + \Delta H_f[\mathrm{AlN}], \quad (6)$$

$$\mu_X = \mu_{X[\mathrm{bulk}]} + \frac{1}{3}\Delta H_f[X_3N_2], \quad (7)$$

for N-rich limit.

III. RESULTS AND DISCUSSION

A. Native defects

In order to find the possibility of compensation, we perform a comprehensive study on the native point defects in AlN. Figure 1 shows the formation energies of native defects in w-AlN as a function of the Fermi level under the two extreme conditions: the Al-rich limit and the N-rich limit. Here, E_F spans the theoretical band gap (5.98 eV).

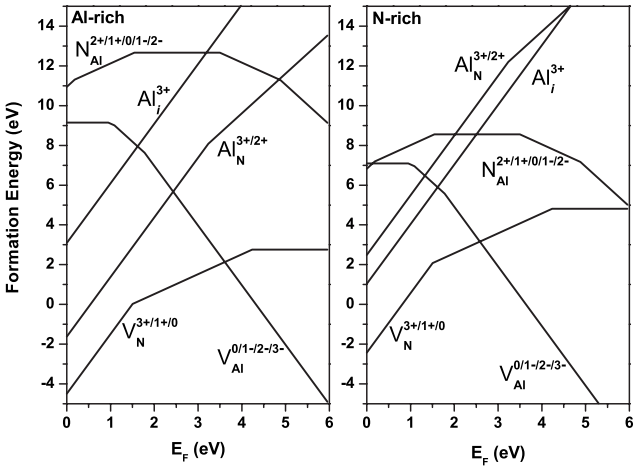

FIG. 1. Defect formation energies for native point defects in *wurtzite* AlN as a function of the Fermi level (E_F) under aluminum-rich (left panel) and nitrogen-rich (right panel) conditions. E_F is defined to be zero at the valence-band edge.

Moreover, V_{N} behave as donors that can donate one, two, or three electrons, but only the V_{N}^{+} and V_{N}^{3+} charge states are stable. The V_{N}^{2+} state is unstable, thus presenting a negative-U effect. The similar behavior of V_{N} has been found in GaN.[20] The V_{N}^{3+} has very low formation energy under p-type conditions (E_F close to the top of the valence band). Taking no account of ionization level, nitrogen vacancies, therefore, are likely to play an important role in compensating acceptors in p-type AlN. Under n-type conditions (E_F close to the bottom of the conduction band), however, the formation energy of V_{N} is actually quite high. In thermodynamic equilibrium, the concentration of nitrogen vacancies should therefore be quite low. On the other hand, V_{N} act as deep donors and the transition level locates at $\epsilon(1+/0)=1.75$ eV blow the conduction-band minimum. This conclusion is different from what was reported about V_{N} in *zinc blend e* AlN in Van de Walles' work,[21] where V_{N} act as a shallow donor. Because of deep transition energy and high formation energy under n-type conditions, V_{N} should not be responsible for the observed n-type conductivity in as-grown AlN. It is more possible that unintentional impurities lead to n-type conductivity other than native defects do. It has been reported that unintentional impurities such as oxygen and silicon are the cause of the observed unintentional n-type doping in GaN.[22] As shown in Fig. 1, the formation energies of V_{N} can be changed significantly depending on growth conditions (Al rich or N rich).

Our calculations reveal that V_{Al} are the lowest-energy defects in n-type AlN, where they behave as triple acceptors. These defects are likely to act as compensating centers for shallow donors. The calculated transition energy $\epsilon(0/-)$ for V_{Al} is 0.95 eV above the valence-band maximum (VBM). Additionally, for p-type AlN, our results show that $\mathrm{Al_N}^{3+}$ has a low formation energy in Al rich, but in N rich, it is very

TABLE I. Atomic radius R_a of X and Al, Pauling electronegativity χ of X, percentage change of bond lengths with respect to bulk AlN, lattice relaxation energy E_{rel}, optimal formation energy (N-rich conditions) for different charge states q, and ionization levels $\epsilon(0/-1)$ for substitutional Be, Mg, and Ca at Al site in AlN.

AlN:X	R_a (Å)	χ	q	X-N(I) (%)	X-N(II) (%)	E_{rel} (eV)	E^f (eV)	ϵ (eV)
X=Be	1.05[a]	1.5[b]	0	−4.1	−0.0	0.18	2.39	0.48
			−1	−2.6	−3.9	0.28	−3.08	
X=Mg	1.50[a]	1.2[b]	0	6.8	8.4	0.68	2.56	0.58
			−1	6.5	7.8	0.78	−2.82	
X=Ca	1.81[a]	1.0[b]	0	13.5	12.0	3.44	3.73	0.95
			−1	14.9	17.4	3.73	−1.27	
X=Al	1.25[a]	…	…	…	…	…	…	…

[a]See Ref. 23.
[b]See Ref. 25.

high, which indicate that Al_N^{3+} concentration is affected by growth conditions of AlN strongly. The other native defects, such as Al_i and N_{Al}, possess high formation energies both in Al rich and N rich, so they cannot be the dominant defects in *w*-AlN.

B. *p*-type doping

In this section, we study the doping behavior of Be, Mg, and Ca impurities in AlN. The main information about the geometry and stability of substitutional impurities is given in Table I.

1. Mg dopant in AlN

In *wurtzite* AlN, a substitutional impurity has four nearest neighbors. One of them located along the *c* axis relative to the impurity (forming X-N(I) bond) is nonequivalent by symmetry to the three remaining neighbors (forming X-N(II) bonds). For substitutional Mg, we find that Mg atom is located very close to the lattice site of the Al atom that it replaces. Lattice relaxation increases the length of Mg-N bonds and releases elastic energies for both neutrally and negatively charged states (listed in Table I). This outward relaxation can be attribute to that of the atomic radius of a substitutional impurity (Mg) which is larger than that of replaced host atom (Al).[15] Large relaxation of the surrounding host atoms will raise the formation energy. Very similar results are obtained for substitutional Mg in *zinc blend e* AlN.[21] Magnesium on the Al site induces the acceptor level $\epsilon(0/1-)=0.58$ eV above the VBM, which is close to the experimental value of 0.51 eV.[23] The large acceptor level of Mg_{Al} may has relation to the electronegativity of Mg atom (for detailed analysis, see below Be dopant in AlN). As can be seen in Fig. 2, Mg_{Al} has a high formation energy. This high formation energy stems from the strict solubility limit imposed by the formation of Mg_3N_2. The formation energy of Mg_{Al} is affected by the growth conditions: by moving from Al-rich to N-rich conditions, the formation energy of Mg_{Al} decreases by $\frac{1}{3}|\Delta H_f[\mathrm{AlN}]|$.

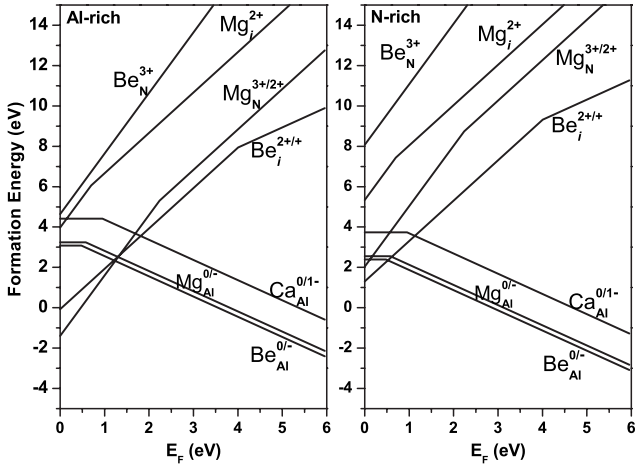

FIG. 2. Formation energy as a function of Fermi level for Mg, Be and Ca in AlN under aluminum-rich (left panel) and nitrogen-rich (right panel) conditions.

In contrast to the Mg_{Al}, Mg_N induces a deep donor level. For Al rich, our calculations indicate that incorporation of Mg on nitrogen site is energetically favorable in *p*-type conditions, which can result in self-compensation effect, but this is not true under N-rich conditions. Therefore, N-rich growth conditions can restrict Mg_N concentration in AlN. Mg on interstitial site behaves as donor, but both in Al- and N-rich conditions, Mg_i is unfavorable due to the large atom size of Mg.

2. Be dopant in AlN

For a substitutional Be_{Al} acceptor, the Be-N bonds show inward relaxation for both neutrally and negatively charged states for Al atom that has larger atomic radius than that of Be. A similar inward relaxation for this complex is also reported in GaN,[19] but percentage change of Be-N bond length is larger than that of Be impurity in AlN due to even larger atomic radius (1.30 Å) (Ref. 24) of Ga atom. The relaxation energy E_{rel} of Be_{Al} is lower than that of Mg_{Al} both in neutrally and negatively charged states, showing that Be replaces Al in AlN with less perturbation of the lattice. Our formation energy calculations reveal that Be occupying Al site creates a single acceptor state above the VBM of AlN. The calculated transition energy of Be_{Al} is 0.48 eV which is shallower than that of Mg_{Al} by ~0.1eV. By using effective-mass theory, Mireles and Ulloa estimated this value to be 0.22–0.45 eV,[25] but their computation is semiempirical and results are affected by computational parameters strongly. In GaN, Latham *et al.* had reported that the acceptor level of Mg_{Ga} was about 0.09 eV higher than that of Be_{Ga},[19] which is in good agreement with our result. Different transition energies between Be_{Al} and Mg_{Al} can be understood as follows: The acceptor level of Mg_{Al} and Be_{Al} consists mostly of *p* orbital. Comparing with Mg, Be atom has lower *p* orbital energy for it is more electronegative;[26] thus, electron can be excited from the VBM to acceptor level with less energy. As can be seen from Fig. 2, the formation energy of Be_{Al} is about 0.2 eV lower than that of Mg_{Al}. So the concentration

of substitutional Be in AlN is expected to be higher than that of Mg. Similarly to substitutional Mg, the formation energy of Be_{Al} is affected by growth conditions.

It is reported that Be_{Ga} acceptor is strongly compensated by interstitial defects,[19] so we pay more attention to Be_i for Be in AlN. According to total energy computation, we find that the lowest-energy structure is that Be atom lies in the center of the hexagonal channel as viewed along the *c* axis. Be_i behaves as donor and can occur in 1+ and 2+ charge states, while only 2+ charge state is stable for Be_i in GaN.[19] This difference is due to the fact that AlN has larger band gap than GaN does. For N-rich conditions, Be_i^{2+} has a low formation energy in *p*-type AlN, $E^f < 0$ eV for E_F at the VBM. So holes may be compensated by interstitial defects Be_i, which is consistent with Be_i in GaN. However, under N-rich conditions, Be_i is energetically unfavorable due to a positive formation energy (E_f=1.30 eV for E_F=0); it is possible to select N-rich growth conditions to restrict the compensation by Be_i in *p*-type AlN.

Since Be_N defect has a high formation energy both in Al- and N-rich conditions, and is thus unlikely to occur in significant concentration, we do not discuss it in detail here.

3. Ca dopant in AlN

Finally, the behaviors of Ca in AlN are discussed. Calcium has the largest atomic radius and is the least electronegative among the three dopants, so it is expected that calcium on a substitutional Al site will produce the most significant outward relaxation with large relaxation energy, highest formation energy, and deepest acceptor level. Our calculations confirm these predictions perfectly. The surrounding N atoms undergo a significant outward relaxation, increasing the Ca-N distance to 2.16 Å. This distance is very close to the Ca-N distance in the compound Ca_3N_2.[27] Similar to Be and Mg, Ca_{Al} behaves as a single acceptor, but the transition level between 0 and −1 charge states occurs around 0.95 eV above the VBM, becoming a deep acceptor. The formation energy of Ca_{Al} is higher than that of both Be_{Al} and Mg_{Al}. So the doping efficiency of Ca is lowest comparing with Be and Mg.

IV. CONCLUSIONS

DFT generalized gradient approximation is used to study the native and group-IIA elements related defects in *wurtzite* AlN. Both V_N and Be_i act as donor with a low formation energy, making them a likely compensating center in the case of acceptor doping. However, V_N do not account for the observed *n*-type conductivity of as-grown AlN for its high ionization levels and high formation energy in *n*-type AlN. Under Al-rich growth conditions, Mg_N and Be_i will compensate hole severely, whereas this problem can be improved by N-rich growth conditions. Our calculations revealed that atomic size and electronegativity of group-IIA impurity are important factors for *p*-type doping efficiency: an impurity with similar atomic radius as Al atom can achieve a higher concentration; an impurity with more electronegative properties can produce a lower ionization level. Among the three elements, Be may be the best candidate for producing *p*-type AlN. In order to achieve high doping efficiency, restricting the concentration of V_N and Be_i is essential and N-rich growth conditions are expected.

ACKNOWLEDGMENTS

This work was supported by the National Natural Science Foundation of China under Project No. 60532090. The authors would like to thank the Supercomputer Center of Shenzhen University for the computation support. The authors also thank R. S. Zheng for useful discussions.

*hbniu@szu.edu.cn

[1] R. J. Molnar, R. Singh, and T. D. Moustakas, Appl. Phys. Lett. **66**, 268 (1995).
[2] S. Nakamura, M. Senoh, and S. Nagahama, Jpn. J. Appl. Phys., Part 2 **35**, L74 (1995).
[3] B. W. Lim, Q. C. Chen, J. Y. Yang, and M. Asif Khan, Appl. Phys. Lett. **68**, 3761 (1996).
[4] K. B. Nam, M. L. Nakarmi, J. Li, J. Y. Lin, and H. X. Jiang, Appl. Phys. Lett. **83**, 2787 (2003).
[5] E. Kuokstis, J. Zhang, Q. Fareed, J. W. Yang, G. Simin, and M. Asif Khan, Appl. Phys. Lett. **81**, 2755 (2002).
[6] I. Vurgaftman and J. R. Meyer, J. Appl. Phys. **89**, 5815 (2001).
[7] Y. Taniyasu, M. Kasu, and T. Makimoto, Nature (London) **441**, 325 (2006).
[8] S. B. Zhang, S. H. Wei, and A. Zunger, J. Appl. Phys. **83**, 3192 (1998).
[9] C. Liu and J. Y. Kang, Opt. Mater. **23**, 169 (2003).
[10] Z. H. Xiong, F. Y. Jiang, Q. X. Wang, and J. P. Rao, Trans. Nonferrous Met. Soc. China **16**, s854 (2006).
[11] S. Nakamura, T. Mukai, and M. Senoh, Jpn. J. Appl. Phys., Part 2 **31**, L139 (1992).
[12] L. E. Ramos, J. Furthmuller, J. R. Leite, L. M. R. Scolfaro, and F. Bechstedt, Phys. Rev. B **68**, 085209 (2003).
[13] P. Blaha, K. Schwarz, G. K. H. Madsen, D. Kvasnicka, and J. Luitz, computer code WIEN2K, Vienna University of Technology, 2002, improved and updated UNIX version of the original; P. Blaha, K. Schwarz, P. Sorantin, and S. B. Trickey, Comput. Phys. Commun. **59**, 399 (1990).
[14] J. P. Perdew, K. Burke, and M. Ernzerhof, Phys. Rev. Lett. **77**, 3865 (1996).
[15] W. J. Lee, J. Kang, and K. J. Chang, Phys. Rev. B **73**, 024117 (2006).
[16] S. Petit, R. Jones, M. J. Shaw, P. R. Briddon, B. Hourahine, and T. Frauenheim, Phys. Rev. B **72**, 073205 (2005).
[17] J. Li, K. B. Nam, M. L. Nakarmi, J. Y. Lin, and H. X. Jiang, Appl. Phys. Lett. **83**, 5163 (2003).
[18] C. G. Van de Walle and J. Neugebauer, J. Appl. Phys. **95**, 3851 (2004).
[19] C. D. Latham, R. M. Nieminen, C. J. Fall, R. Jones, S. Öberg, and P. R. Briddon, Phys. Rev. B **67**, 205206 (2003).

[20] C. H. Park and D. J. Chadi, Phys. Rev. B **55**, 12995 (1997).
[21] C. Stampfl and C. G. Van de Walle, Phys. Rev. B **65**, 155212 (2002).
[22] C. G. Van de Walle, C. Stampfl, and J. Neugebauer, J. Cryst. Growth **189/190**, 505 (1998).
[23] K. B. Nam, M. L. Nakarmi, J. Li, J. Y. Lin, and H. X. Jiang, Appl. Phys. Lett. **83**, 878 (2003).
[24] http://www.webelements.com/webelements/elements/text/periodic-table/radii.html
[25] F. Mireles and Sergio E. Ulloa, Phys. Rev. B **58**, 3879 (1998).
[26] A. García and M. L. Cohen, Phys. Rev. B **47**, 4221 (1993).
[27] J. Neugebauer and C. G. Van de Walle, J. Appl. Phys. **85**, 3003 (1999).